Sensors and Actuators B 215 (2015) 146–151

Contents lists available at ScienceDirect

Sensors and Actuators B: Chemical

journal homepage: www.elsevier.com/locate/snb

Micro/nano optical fibers for label-free detection of abrin with high sensitivity

Guigen Liu[a,*], Kaiwei Li[b]

[a] Department of Electrical Engineering, University of Nebraska-Lincoln, Lincoln, NE 68588, USA
[b] State Key Laboratory of Applied Optics, Changchun Institute of Optics, Fine Mechanics and Physics, Chinese Academy of Sciences, Changchun 130033, China

ARTICLE INFO

Article history:
Received 4 January 2015
Received in revised form 8 March 2015
Accepted 26 March 2015
Available online 2 April 2015

Keywords:
Micro/nano optical fibers
Biosensors
Label-free assay
Abrin detection

ABSTRACT

The recognition of abrin is of great civil and military importance. As an alternative to general detecting techniques, such as enzyme-linked immunosorbent assay (ELISA) and electrochemiluminescence (ECL)-based assay, micro/nano optical fibers (MNFs) for the label-free detection of abrin have been investigated for the first time in this paper. The MNFs fabricated through chemical etching are robust and have excellent mechanical strength for practical applications. This MNF-based biosensors feature fast response, high sensitivity, and low cost. A limit of detection of 10 pg/mL was obtained using a MNF with a waist diameter of circa 1.0 μm, and the typical measurement time was less than 10 min. By taking advantage of the label-free detection, Langmuir kinetics fitting for the dynamic reaction curve suggested a large affinity constant between the antibody and abrin. Regeneration ability of the sensor was also demonstrated by the maintenance of high sensitivity and selectivity after releasing experiments.

1. Introduction

The attractive rosary beans have been used to make jewellery (such as necklaces, rosaries, earrings, etc.) since ancient times [1,2]. Despite the charming appearance, they are also notorious for the high toxicity of an inner ribosome inactivating protein known as abrin. Abrin inhibits protein synthesis and results in eventual cell death, which can be developed as chemical weapons by terrorists [3–6]. The 50% inhibitory concentration of abrin for protein synthesis is 0.4 ng/mL [7], resulting in the LD_{50} (50% lethal dose) values of 20 μg/kg for mouse [8] and the estimated fatal dose for humans is 0.1–1 μg/kg body weight [9]. However, no antidote or vaccine for abrin has been reported except a neutralizing antibody inhibiting abrin toxicity both in vitro and in vivo [10]. Therefore, the rapid detection of abrin with a high sensitivity has been the investigation focus for many researchers.

To date, several methodologies for distinguishing abrin have been reported. Tang et al. showed a limit of detection (LOD) of 1 nM based on DNA aptamer [5]. Owens and Koester obtained the detection of abrin dissolved in various beverages at 500 ng/mL level using liquid chromatography/tandem mass spectrometry (LC/MS) [11]. Garber et al. applied enzyme-linked immunosorbent assay (ELISA) and electrochemiluminescence (ECL)-based assay to fulfill detection of abrin in buffer solution with a concentration as low as 0.1–0.5 ng/mL [6] or 0.03–1.3 μg/mL in original food samples [12]. Recently, Zhou et al. realized the detection of 0.5 ng/mL abrin in phosphate buffered saline by resort to monoclonal antibody-based sandwich-type ELISA [13]. LC/MS is a time-consuming and expensive method, ELISA is laborious with multiple manual manipulations and needs chemical labels, ECL and DNA aptamer-based detection are only limited to laboratory scientific research. Therefore, the development of a fast, cost-effective, point-of-care, highly sensitive, and label-free immunosensor to accomplish abrin detection is of great importance, both in civil engineering and military applications.

Among various potential biodetection techniques to accomplish the abovementioned mission, such as surface acoustic, cantilever, quartz crystal microbalance and optical devices, the optical biosensors are a promising and powerful tool [14], especially those based on optical fibers which are capable of remote sensing, immune to electromagnetic interference, able to realize multiplexed detection, etc. [15–18]. Over the last decade, micro/nano optical fibers (MNFs) have attracted great research attention since its low-loss fabrication techniques were investigated [19,20]. Till now, a variety of biochemical sensors based on MNFs have been reported, such as fast response hydrogen sensor [21], surface absorption spectroscopy [22], and absorption detection of bovine serum albumin (BSA) in a microfluidic chip [23]. Most recently, we have reported

* Corresponding author. Tel.: +1 4026172678.
E-mail address: guigenliu@hotmail.com (G. Liu).

http://dx.doi.org/10.1016/j.snb.2015.03.056
0925-4005/

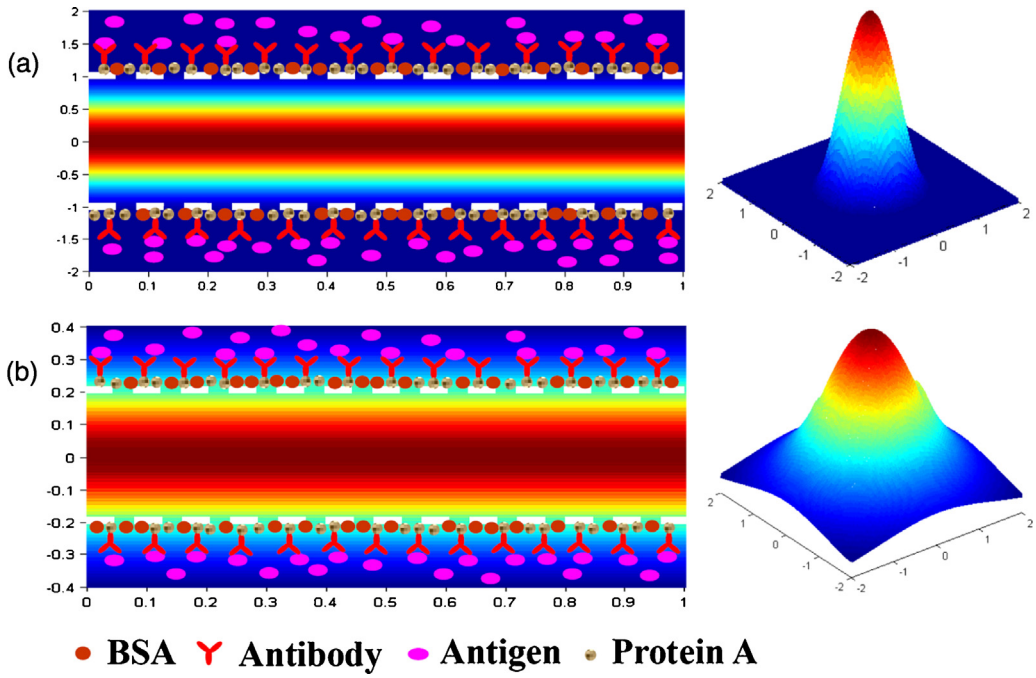

Fig. 1. Schematic showing the optical fiber with a diameter of (a) 2 μm and (b) 0.4 μm for biosensing along with the calculated power distribution of fundamental mode. Other parameters used in the calculations are $\lambda = 648$ nm, $n_{co} = 1.45$, and $n_{cl} = 1.333$. The core boundaries are designated by the white dash lines, the right column exhibits the according power distribution over the cross section. For all axes, the unit is μm.

on the detection of cancer biomarker in serum using an optical microfiber amplified by gold nanoparticles [24]. Given the merits of ultra high sensitivity, fast response, cost-effective detection and tiny footprint, the promising MNF biosensors have been explored to recognize abrin based on a label-free manner in this paper.

2. Sensing properties of MNFs

MNFs are optical fibers with a waist diameter of around 1 μm or smaller. With such a smaller diameter, they are operated at or close to single-mode condition [25]. The bound modes supported by an optical fiber is determined by the V-number expressed as [26]

$$V = \frac{2\pi r}{\lambda}\sqrt{n_{co}^2 - n_{cl}^2} \quad (1)$$

where r, λ, n_{co} and n_{cl} are radius, wavelength, core refractive index (RI) and cladding RI, respectively. When $V < 2.405$, only the fundamental mode can be propagated without attenuation, which is the so-called single-mode condition. One important advantage of single-mode operation over multimode scheme is the much more stable response, because multimode interference will induce fluctuation of the output intensity of the tapered fiber as external RI (or pathogen concentration) varies [27,28].

Another important merit of MNFs concerning highly sensitive biodetection is the large power fraction in the evanescent field which interacts directly with the analyte. As shown in Fig. 1(a), an optical fiber with a diameter of 2 μm only has weak evanescent field for detecting biomolecules. In contrast, for a 0.4-μm-thick MNF in Fig. 1(b), a strong evanescent field penetrates into the sample under detection, facilitating recognition of targets with a much higher sensitivity. As explicitly shown by Fig. 1(b), the biomolecules are well within the strong evanescent field of the fundamental mode, hence intensifying the interaction between optical signal and targets.

3. Materials and methods

3.1. Materials

The pristine SMF-28e optical fibers were purchased from Corning. Glutaraldehyde, 3-aminopropyl-triethoxysilane (APTES), phosphate buffer saline (PBS), and bovine serum albumin (BSA) were all purchased from Sigma–Aldrich. Abrin and rabbit-anti-abrin antibody were obtained from research institute of chemical defense of Chinese People's Liberation Army. Deionized water was derived from a Milli-Q water purifying system.

3.2. Experimental arrangement

Our experimental setup is shown in Fig. 2. It consists of a couple of simple optical elements: a red LED with a maximum output power of 3 W which was driven by a home-made circuit with tunable luminance, a 40× microscope objective lens for focusing, two FC adapters holding two ends of the biconically tapered optical sensing fibers, and a home-made micro optical fiber spectrometer which was connected to a PC for data acquisition. Note that power of the LED should be tuned to a certain value before tests so that the output power of the tapered fiber is neither too high (otherwise saturated) nor too low to obtain a good

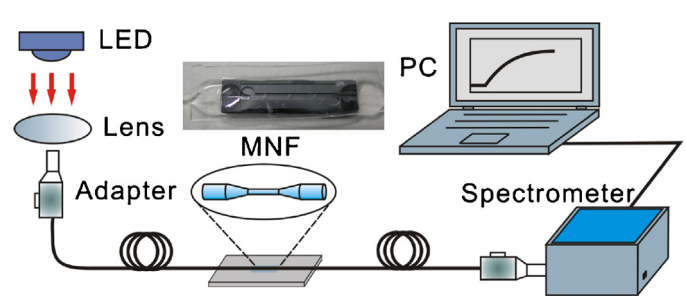

Fig. 2. Experimental setup. Inset shows the photograph of a sample cell.

signal-to-noise ratio. A LED with lower maximum power may be feasible to reduce energy consumption; however, a finer adjustment of light injection is necessary. The straight MNF was located in a silicon micro-chamber fabricated through MEMS (micro-electro-mechanical systems) technology [29]. The inset in Fig. 2 shows a photograph of the sample chamber covered by a polydimethylsiloxane (PDMS) film. In such a way, the mechanical stability of the MNF is protected.

3.3. MNF fabrication

There are two basic methods for fabricating MNFs, one is heat drawing [19,20,30] and the other is chemical etching through hydrofluoric acid [31,32]. The heat drawing method features fast fabrication, low surface roughness, easy control of taper profile, etc. However, transfer of the MNFs from the drawing apparatus to an accommodating sample cell is inevitable, which necessitates careful manual operations to prevent the tiny MNFs from breaking. In contrast, chemical etching can be done within the etching chamber which also serves as the detection cell, although it is slower and may produce MNFs with rougher surface than the drawing method does. The chemical etching method does not need a transfer process for the fabricated MNFs and thus extremely reduces the possibility of breaking. Furthermore, as shown later, the MNFs well fabricated by chemical etching can have very smooth surface and possess low enough optical losses to facilitate our biorecognition experiments. Therefore, the chemical etching was used in this work.

In order to obtain smooth MNFs, acetic acid (CH_3COOH) was added as a buffer in the fabrication process [29]. The acetic acid provided a bunch of H^+ which contributed to a gentle etching process and thus led to a better surface quality. The etching procedure was monitored by a simple transmission measurement setup and stopped by rinsing extensively when the output power was reduced to a certain value which corresponded to a certain waist diameter.

3.4. Functionalization

In order to guarantee the selectivity of the MNF biosensors, the specific antibody was immobilized onto the fiber surface and the blank sites were blocked by BSA. It took a couple of steps to functionalize the MNF according to [33]: (1) *Cleaning*: The manufactured MNF was cleaned by piranha solution (hydrogen peroxide and 6 M sulfuric acid with a volume ratio of 3:7) for 10 min and then rinsed with boiled deionized water. The cleaning procedure created reactive hydroxyl groups on the fiber surface. (2) *Silanization*: The solution of 5% (v/v) APTES in methanol was added to silanize the cleaned optical fiber for 15 min, which left a free amine terminal for further reaction. (3) *Activation*: An aqueous solution of 2.5% glutaraldehyde was applied to treat the aminated surface. The glutaraldehyde had two aldehydes at the two sides, one interacted with the amine terminal, and the other was left on the surface for the following covalent binding of biomolecules. (4) *Protein A coating*: The protein A with a concentration of 40 μg/mL was added to modify the fiber surface for 1 h, the coating of protein A helped the immobilization of antibody with a uniform direction and thus keep the activity of antibody to a maximum extent. (5) *Antibody immobilization*: The rabbit-anti-abrin antibody in PBS with a concentration of 200 μg/mL was added to covalently link to aldehyde groups on the silanized surface for about 1 h. (6) *Blocking*: The left blank sites might cause significant nonspecific binding, therefore, BSA with a concentration of 10 mg/mL was introduced to block the blank sites to minimize nonspecific absorption. After these six steps, the MNF immuno-sensors were formed and ready for biorecognition with selectivity.

3.5. Binding and release experiments on abrin

After functionalization, the sensor was utilized to selectively bind the target abrin molecules. An abrin stock solution was serially diluted to different concentrations (10 pg/mL, 1 ng/mL, and 100 ng/mL) using deionized water. The output intensity was recorded for reference when the tapered fiber was surrounded by deionized water. After 10-min reaction for an abrin concentration and collection of the spectrum change, the solution was switched to another higher concentration. The same procedure was repeated until all the abrin solutions were measured. Due to the small volume of the sample cell, only ~100 μL of abrin aqueous solution was needed for each concentration to fill the silicon micro-chamber.

In order to investigate the ability of regeneration, release experiments were carried out. After the serial detections of abrin, regeneration buffer solution (10 mM glycine-HCl, pH 2.3) was loaded to remove the antigen from the antibody. After the first release, 100 ng/mL abrin solution was added to test its recognition ability. Then, the second release experiment was carried out after which BSA solution with a concentration of 100 ng/mL was added to verify its specificity after regeneration. At last, a third release experiment was performed, after which the detection of abrin with a low concentration of 10 pg/mL was performed. The third release experiment is used to investigate the viability of abrin detection with high sensitivity after several releases.

4. Results and discussion

4.1. Sensing fiber characterization

A chemically fabricated MNF with a waist diameter of around 1.2 μm is shown by the scanning electron microscope (SEM) image in Fig. 3(a), which exhibits smooth fiber surface and a uniform radius. In order to test the flexibility and mechanical strength of the sensing fiber fabricated through our chemical etching, another fiber with a diameter of around 15 μm was manipulated under an optical microscope to form a knot with a smallest bend radius of circa 450 μm, as shown by the SEM image in Fig. 3(b). Survival of the fiber knot suggests that the sensing fiber is robust and can be fixed into compact devices.

4.2. Antibody immobilization

Results of the monitored transitive immobilization process of antibody on the MNF with a waist diameter of circa 1.0 μm are shown in Fig. 4. Evolution of the spectrum recorded in Fig. 4(a) indicates that the overall intensity decreases as the immobilization of antibody proceeds, however, the variation rate decreases as time goes on, indicating a saturation will be reached. Due to the narrowband spectrum of the red LED used in the experiments, the collected spectra show peak wavelengths at around 648 nm (as shown in Fig. 4(a)). To visualize the temporal transition, the normalized intensity at three different wavelengths (i.e. 640, 648 and 653 nm designated in Fig. 4(a)) as a function of time is plotted in Fig. 4(b). It is apparent to see that the immobilization process tends to saturate as time passes by, which is a typical Langmuir kinetics behavior.

It is of great interest to investigate the kinetics during antibody immobilization, which could help quantitatively compare the efficiency of different modification methodologies. The response exhibits exponential decay behavior which is similar to the adsorption process often referred as Langmuir kinetics. The Langmuir kinetics model can be expressed as [34]:

$$\theta = 1 - \exp(-k_{obs}t) \quad (2)$$

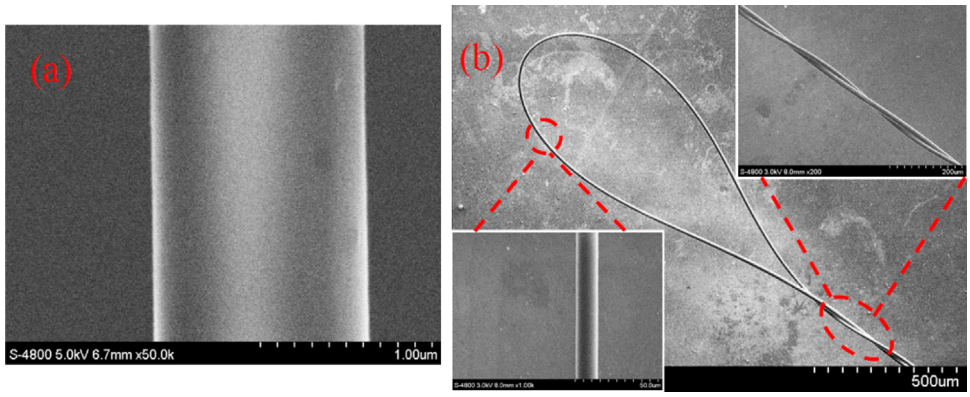

Fig. 3. Scanning electron microscope images of (a) a fabricated 1.2-μm-thick MNF showing smooth and uniform waist and (b) a knot formed by a 15-μm-thick fiber with a smallest bend radius of circa 450 μm.

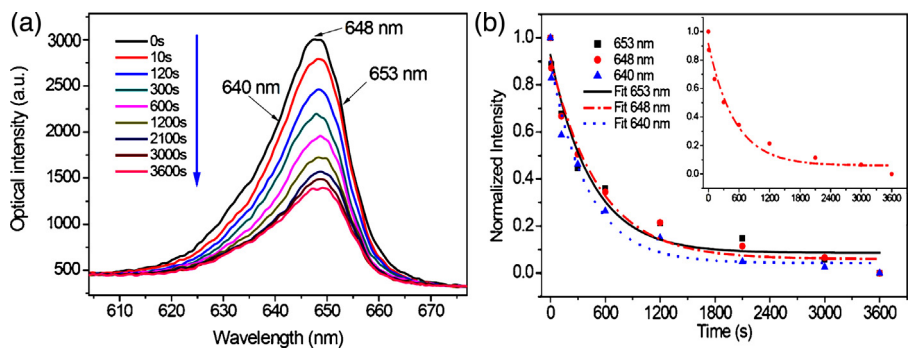

Fig. 4. Output (a) spectrum and (b) normalized intensity at three fixed wavelength designated in (a) during the immobilization of antibody. In (b), discrete dots are the experimental data at the three wavelengths, Langmuir kinetics model fitting is performed for each wavelength, inset shows separately the results at 648 nm for clarity.

where θ is the fractional coverage of the reactive sites whose value is between zero and one. The observed binding rate constant k_{obs} is a measure of reaction speed, and a bigger k_{obs} indicates a quicker reaction. Typically, the output intensity of a MNF does not response linearly to external RI [23,32], however, in our biodetection case, we assume that the molecule attachment causes so slight variation in local RI around the MNF that the output intensity responses linearly to the binding of biomolecules. Therefore, the normalized output intensity could be regarded as the portion of residual reactive sites, i.e. $1-\theta$. Thus, according to the output intensity against reaction time as shown by the experimental data in Fig. 4(b) for the three different wavelengths, a Langmuir kinetics fitting is performed for each individual series of data to obtain the constant k_{obs}. For clarity, an inset for the wavelength of 648 nm is shown separately in the upper right corner of Fig. 4(b). Because the attachment process is independent of wavelength, so the obtained k_{obs} values of 2.25×10^{-3}, 1.99×10^{-3}, and $2.44\times10^{-3}\,s^{-1}$ for the wavelength of 653, 648, and 640 nm, respectively, are close. Thus, a mean value of $2.23\times10^{-3}\,s^{-1}$ with a standard deviation (SD) of $\pm0.23\times10^{-3}\,s^{-1}$ is confirmed for the k_{obs} of our antibody immobilization. This value is circa one order of magnitude higher than the one obtained in [34] for the immobilization of BSA antibody although our concentration of antibody is lower, which may be owing to the different antibodies and covalent link chemicals. It is clear to see from the kinetics curves shown in Fig. 4(b) that the immobilization tends to saturate after 1 h.

4.3. Abrin detection in aqueous samples

The antibody-modified MNF was used to detect abrin in aqueous solutions prepared with different concentrations. The spectrum change after 10-min reaction for each concentration is shown in Fig. 5(a). Apparently, the LOD as low as 10 pg/mL is verified. Note that the spacing between adjacent samples shrinks as abrin concentration increases, which indicates the approaching of saturation. The obtained LOD of the MNF biosensor for abrin detection is at least one order of magnitude lower than those of other techniques summarized in the introduction part. In addition, the reaction tends to saturate within the first 5 min and almost finishes within 10 min, which proves that our MNF biosensors have the advantage of fast detection.

Still, a Langmuir kinetics fit done for the 10 pg/mL abrin within 10 min at a wavelength of 648 nm as shown in Fig. 5(b). The obtained k_{obs} is $1.3\times10^{-2}\,s^{-1}$ which is nearly one order of magnitude higher than that of the immobilization process. Note that the abrin concentration is over 7 orders of magnitude lower than that of the antibody, indicating the binding of abrin to antibody is much faster than antibody to the fiber surface. This could be attributed to different reaction mechanisms, while chemical reactions govern the antibody immobilization, the antigen–antibody reaction belongs to some physical binding forces, including hydrogen bond, Van der Waals' force, electric charge effect and hydrophobic interaction [35]. Furthermore, the antibody molecules are much larger than abrin, which means the transportation of antibody to fiber surface is much slower than the binding of abrin to antibody. This result proves the high affinity between the antibody and abrin.

4.4. Regeneration ability

One important aspect of biosensors is the regeneration ability. Regeneration ability of our MNF biosensor is revealed by the release experiments described in Section 3.5, the results are shown in Fig. 6. The response to 100 ng/mL abrin after the first release is shown in Fig. 6(a), the 5-min reaction results in an obvious drop in the

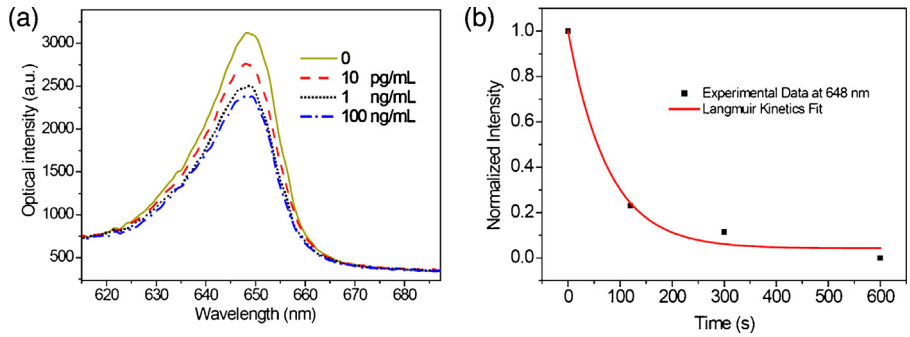

Fig. 5. (a) The spectrum response to abrin aqueous samples after 10-min reaction, and (b) normalized intensity versus time for the concentration of 10 pg/mL at 648 nm (peak wavelength).

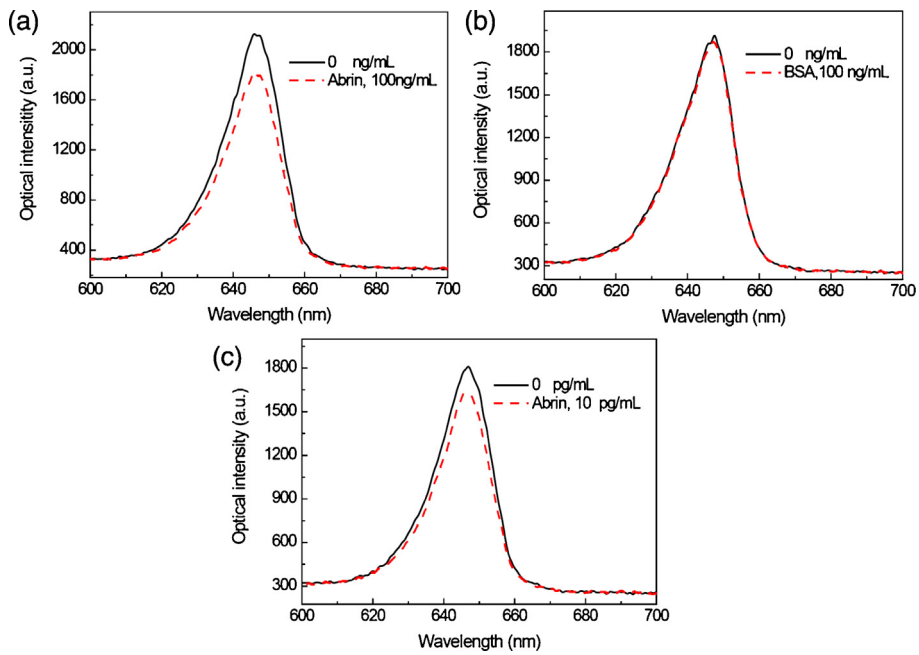

Fig. 6. Release experiments. Detection of (a) 100 ng/mL abrin after the first release, (b) 100 ng/mL BSA after the second release, and (c) 10 pg/mL after the third release.

spectrum, and this experiment concludes that the MNF biosensor still conserves a great activity after the releasing process. However, the biosensor shows only neglectable response to BSA solution with the same concentration of 100 ng/mL within 5 min after the second release (Fig. 6(b)), from which one can conclude that the selectivity is maintained after releasing. After the third release experiment, the MNF biosensor conserves high sensitivity for abrin detection, which is verified by the easily detectable change in the spectrum after the detection of 10 pg/mL abrin for 10 min (Fig. 6(c)). These experiments prove that high sensitivity and selectivity are maintained upon releases, indicating good regeneration ability.

Note that the saturation phenomenon is also witnessed after the release experiments. Although there is a four-order-of-magnitude difference between the concentrations in Fig. 6(a) and (c), the spectrum change in Fig. 6(c) is only slightly lower than that in Fig. 6(a). The reason is that saturation blocks the further response when high abrin concentration is detected, which reveals that the dynamic range is limited for such a high-sensitivity biosensor.

Finally, results of the regeneration experiments in Fig. 6(a) and (c) along with the previous results in Fig. 5(a) also suggest that the developed MNF biosensor for label-free detection of abrin is repeatable.

5. Conclusions

The fast detection of abrin using MNFs was first realized with a LOD of 10 pg/mL within a typical reaction time of less than 10 min. Compared to well-established techniques for abrin, such as ELISA, ECL, LC/MS, etc., the MNF biosensors are superior in terms of detection limit and detection time. By taking advantage of the label-free detections, Langmuir kinetics fittings of the antibody immobilization and antibody–antigen binding processes can be performed on the experimental data monitored on-line, which reveals that the binding process is much faster than the immobilization transition and thus testifies a strong affinity between the antibody and abrin. Finally, the regeneration ability is well confirmed by the good conversation of high sensitivity and specificity after release experiments.

Acknowledgements

Much of the work was done when G. Liu was with Changchun Institute of Optics, Fine Mechanics and Optics (CIOMP), Chinese Academy of Sciences (CAS). Helpful discussions and supports from Prof. Yihui Wu at CIOMP are highly appreciated. The authors also acknowledge the help on biological experiments from Dr. Zhiqiang

Zhang with Suzhou Institute of Biomedical Engineering and Technology, CAS.

References

[1] S. Olsnes, The history of ricin, abrin and related toxins, Toxicon 44 (2004) 361–370.
[2] E.G.C. Clarke, D.J. Humphreys, The detection of abrin, J. Forensic Sci. 11 (1971) 109–113.
[3] H. Zhou, B. Zhou, H. Ma, C. Carney, K.D. Janda, Selection and characterization of human monoclonal antibodies against abrin by phase display, Bioorg. Med. Chem. Lett. 17 (2007) 5690–5692.
[4] E.A.E. Garber, Toxicity and detection of ricin and abrin in beverages, J. Food Prot. 71 (2008) 1875–1883.
[5] J. Tang, T. Yu, L. Guo, J. Xie, N. Shao, Z. He, In vitro selection of DNA aptamer against abrin toxin and aptamer-based abrin direct detection, Biosens. Bioelectron. 22 (2007) 2456–2463.
[6] E.A.E. Garber, J.L. Walker, T.W. O'brien, Detection of abrin in food using enzyme-linked immunosorbent assay and electrochemiluminescence technologies, J. Food Prot. 71 (2008) 1868–1874.
[7] S. Narayanan, K. Surendranath, N. Bora, A. Surolia, A.A. Karande, Ribosome inactivating proteins and apoptosis, FEBS Lett. 579 (2005) 1324–1331.
[8] K.J. Dickers, S.M. Bradberry, P. Rice, G.D. Griffiths, J.A. Vale, Abrin poisoning, Toxicol. Rev. 22 (2003) 137–142.
[9] F. Stirpe, L. Barbieri, M.G. Battelli, M. Soria, D.A. Lappi, Ribosome inactivating proteins from plants: present status and future prospects, Biotechnology 10 (1992) 405–412.
[10] S. Kalpana, A.K. Anjali, A neutralizing antibody to the A chain of abrin inhibits abrin toxicity both in vitro and in vivo, Clin. Vaccine Immunol. 15 (2008) 737–743.
[11] J. Owens, C. Koester, Quantitation of abrine, an indole alkaloid marker of the toxic glycoproteins abrin, by liquid chromatography/tandem mass spectrometry when spiked into various beverages, J. Agric. Food Chem. 56 (2008) 11139–11143.
[12] E.A.E. Garber, K.V. Venkateswaran, T.W. O'Brien, Simultaneous multiplex detection and confirmation of the proteinaceous toxins abrin, ricin, botulinum toxins, and staphylococcus enterotoxins A, B, and C in food, J. Agric. Food Chem. 58 (2010) 6600–6607.
[13] Y. Zhou, X.-L. Tian, Y.-S. Li, et al., Development of a monoclonal antibody-based sandwich-type enzyme-linked immunosorbent assay (ELISA) for detection of abrin in food samples, Food Chem. 135 (2012) 2661–2665.
[14] X. Fan, I.M. White, S.I. Shopova, et al., Sensitive optical biosensors for unlabeled targets: a review, Anal. Chim. Acta 620 (2008) 8–26.
[15] M.I. Zibaii, H. Latifi, M. Karami, M. Gholami, S.M. Hosseini, M.H. Gheze-layagh, Non-adiabatic tapered optical fiber sensor for measuring the interaction between α-amino acids in aqueous carbohydrate solution, Meas. Sci. Technol. 21 (2010) 105801.
[16] H.I. Balcer, H.J. Kwon, K.A. Kang, Assay procedure optimization of a rapid reusable protein C immunosensor for physiological samples, Ann. Biomed. Eng. 30 (2002) 141–147.
[17] C. Beres, F.V.B. de Nazare, N.C.C. de Souza, et al., Tapered plastic optical fiber-based biosensor-Tests and application, Biosens. Bioelectron. 30 (2011) 328–332.
[18] X.-D. Wang, O.S. Wolfbeis, Fiber-optic chemical sensors and biosensors, Anal. Chem. 85 (2012) 487–508.
[19] L. Tong, R.R. Gattass, J.B. Ashcom, S. He, J. Lou, M. Shen, I. Maxwell, E. Mazur, Subwavelength-diameter silica wires for low-loss optical wave guiding, Nature 426 (2003) 816–819.
[20] G. Brambilla, V. Finazzi, D.J. Richardson, Ultra-low-loss optical fiber nanotapers, Opt. Express 12 (2004) 2258–2263.
[21] J. Villatoro, D. Monzon-Hernandez, Fast detection of hydrogen with nano fiber tapers coated with ultra thin palladium layers, Opt. Express 13 (2005) 5087–5092.
[22] F. Warken, E. Vetsch, D. Meschede, M. Sokolowski, A. Rauschenbeutel, Ultra-sensitive surface absorption spectroscopy using sub-wavelength diameter optical fibers, Opt. Express 15 (2007) 11952–11958.
[23] L. Zhang, P. Wang, Y. Xiao, H. Yu, L. Tong, Ultra-sensitive microfiber absorption detection in a microfluidic chip, Lab Chip 11 (2011) 3720–3724.
[24] K. Li, G. Liu, Y. Wu, P. Hao, W. Zhou, Z. Zhang, Gold nanoparticle amplified optical microfiber evanescent wave absorption biosensor for cancer biomarker detection in serum, Talanta 120 (2014) 419–424.
[25] L. Tong, J. Lou, E. Mazur, Single-mode guiding properties of subwavelength-diameter silica and silicon wire waveguides, Opt. Express 12 (2004) 1025–1035.
[26] A.W. Snyder, J.D. Love, Optical Waveguide Theory, Chapman and Hall, London, 1983.
[27] K. Rijal, A. Leung, P.M. Shankar, R. Mutharasan, Detection of pathogen *Escherichia coli* 0157:H7 at 7 cells/mL using antibody-immobilized bioconical tapered fiber sensors, Biosens. Bioelectron. 21 (2005) 871–880.
[28] A. Leung, K. Rijal, P.M. Shankar, R. Mutharasan, Effects of geometry on transmission and sensing potential of tapered fiber sensors, Biosens. Bioelectron. 21 (2006) 2202–2210.
[29] Y. Wu, X. Deng, F. Li, X. Zhuang, Less-mode optic fiber evanescent wave absorbing sensor: parameter design for high sensitivity liquid detection, Sens. Actuators B 122 (2007) 127–133.
[30] G. Brambilla, F. Xu, P. Horak, Y. Jung, F. Koizumi, N.P. Sessions, E. Koukharenko, X. Feng, G.S. Murugan, J.S. Wilkinso, D.J. Richardson, Optical fiber nanowires and microwires: fabrication and applications, Adv. Opt. Photonics 1 (2009) 107–161.
[31] H.S. Haddock, P.M. Shankar, R. Mutharasan, Fabrication of bioconical tapered optical fibers using hydrofluoric acid, Mater. Sci. Eng. B97 (2003) 87–93.
[32] G. Liu, Y. Wu, K. Li, P. Hao, P. Zhang, M. Xuan, Mie scattering-enhanced fiber-optic refractometer, IEEE Photon. Technol. Lett. 24 (2012) 658–660.
[33] T. Cass, F.S. Ligler (Eds.), Immobilized Biomolecules in Analysis: A Practical Approach, Oxford University Press, London, 1999.
[34] A. Leung, P.M. Shankar, R. Mutharasan, Real-time monitoring of bovine serum albumin at femtogram/mL levels on antibody-immobilized tapered fibers, Sens. Actuators B 123 (2007) 888–895.
[35] E. Harlow, D. Lane, Using Antibodies: A Laboratory Manual, Cold Spring Harbor Laboratory Press, 1999.

Biographies

Guigen Liu received the B.E. degree in mechanical engineering from Qingdao University, Qingdao, China, in 2008, and the Ph.D. degree in mechanical engineering from the Changchun Institute of Optics, Fine Mechanics and Physics (CIOMP), Chinese Academy of Sciences, Changchun, China, in 2013. During his Ph.D. phase, his research focused on tapered optical fibers for label-free biochemical detection. After receiving the Ph.D. degree, he was with CIOMP as a Research Assistant. In 2014, he joined the Department of Electrical and Computer Engineering, University of Nebraska-Lincoln, Lincoln, NE, USA, as a Post-Doctoral Research Associate. His research interest includes fiber-optic biochemical sensors, ultrasound sensors, high-speed temperature sensors, anemometers, etc.

Kaiwei Li received the B.E. degree in mechanical engineering from Jilin University, Changchun, China, in 2009, and the Ph.D. degree in mechanical engineering from the Changchun Institute of Optics, Fine Mechanics and Physics (CIOMP), Chinese Academy of Sciences, Changchun, China, in 2014. During his Ph.D. phase, his research focused on optical micro/nanofiber biosensors for cancer biomarker detection. After receiving the Ph.D. degree, he was with CIOMP as a Postdoctoral Research Fellow. His research interest includes optical micro/nanofiber biosensors, optical fiber SPR sensors and novel microstructured optical fibers, etc.